Minimax Theory and its Applications

Volume 12 (2027), No. 1, 64 to 86

Blockchain-Based Cybersecurity Framework for ECG Classification Using a MiniMax-Normalized Parallel Cell Attention 1D Convolutional Network Optimized by Cuckoo Catfish Algorithm

Seng-Phil Hong

School of Computing and AI, HanShin University, 137, Hanshindae-gil, Osan-si, Gyeonggi-do, Republic of Korea, Email: sphong@hs.ac.kr, ORCID: 0000-0003-4391-7313

Abstract

The high-rate development of intelligent healthcare systems has allowed the automated processing of electrocardiogram (ECG) signals to detect cardiovascular diseases early and monitor patients in real-time. Nevertheless, proper classification without compromising the security and privacy of the data is an essential issue in the contemporary digital healthcare setting. The current ECG analysis structures are usually characterized by noise sensitivity, inefficient feature representation, suboptimal model parameter tuning, and susceptibility to cyberattacks, which inspired the creation of a secure and optimized analytical framework. To overcome these issues, this paper presents a Parallel Cell Attention 1D Convolutional Network with Cuckoo Catfish Optimizer (PCA-1DCN-CCO) embedded into a blockchain-based cybersecurity system to provide trustworthy ECG classification. First, Joint Frame-Level and Block-Level Rate-Perception Optimized Preprocessing (JFL-BLRPOP) improves the quality of signals by increasing the consistency of perceptions and minimizing the distortion of noise. After that, Synchrosqueezing-based Short-Time Fractional Fourier Transform (S-STFFT) is used to extract features discerning discriminative time-frequency properties of ECG signals. A Parallel Cell Attention 1D Convolutional Network is used to classify the extracted features; the Cuckoo Catfish Optimizer is used to tune the model parameters to enhance the efficiency of the learning process. Moreover, a Holistic Blockchain Consensus Spectral Graph Neural Network (HBC-SGNN) will provide security in data management of ECG and cyber-attack detection. Experimenting on the PTB-XL dataset shows that it has higher performance with 99.71% accuracy, 99.64% precision, 99.57% recall, 99.60% F1-score, 99.59% specificity, and the lowest computational latency than current methods. The suggested framework is secure, scalable, and highly precise in terms of intelligent ECG classification and reliable healthcare data management.

Keywords: Blockchain Security, Cardiovascular Disease Detection, Cuckoo Catfish Optimizer, Deep Learning, Electrocardiogram Signal Analysis, Healthcare Data Privacy.

1. Introduction

Intelligent monitoring technology, medical sensors, and data-driven diagnostic services have been embraced at a faster pace due to the swift digitalization of healthcare systems. Physiological signal analysis has turned into an important aspect of the contemporary healthcare service as the demand for constant monitoring of patients and early detection of diseases increases [1-3]. Electrocardiogram (ECG) records are among other biomedical signals that are important in the regulation of cardiac activity and in the diagnosis of cardiovascular abnormalities by clinicians. The adoption of artificial intelligence in medical settings has allowed automatic processing of high amounts of health-related information, enhancing the quality of diagnoses, decreasing the human factor in work, and facilitating the adoption of clinical decision-making in time [4-5]. Nonetheless, the growing dependence of digital healthcare infrastructures has also come with grave issues concerning data privacy, safe communication, and the defense against developing cyber threats, especially when interconnectedness is involved, and sensitive patient data is continuously created and shared.

The current healthcare systems are becoming more and more reliant on distributed networks, wearables, and cloud storage services in order to process patient data effectively. These technologies make them more accessible, allowing access to remote healthcare services and monitoring health in real-time [6-8]. Even with these benefits, they also have major cybersecurity weaknesses, such as hacking, data rewriting, and service outage attacks. Medical records are very confidential, and any breach of confidentiality can affect patient safety, institutional credibility, and breach of regulations. Traditional centralized storage systems tend to be less transparent and reliable due to the fact that a single failure will expose all the data to cyber threats. As a result, the development of strong, reliable, and safe data control systems has become one of the primary concerns in the research and development of smart healthcare [9-10].

The blockchain technology has received significant focus as a secure system of managing healthcare data because it is a decentralized and non-alterable structure. Transparency, traceability, and data integrity are improved through the spread of data records among various participants and through transaction verification by all parties to the blockchain. It allows safe sharing of data in healthcare settings and maintains ownership of patients, and also controlled access to medical data [11-12]. The blockchain records are immutable, which increases the credibility of the stakeholders and decreases the chance of unauthorized alteration of the data. These attributes make blockchain a prospective base for enhancing cybersecurity and providing secure data transfer in data-intensive medical systems.

At the same time, recent developments in deep learning have substantially enhanced automated analysis of various biomedical signals, including ECG signals, by training more complex temporal and morphological patterns on large datasets. The ability to assist in making accurate disease forecasts and smart healthcare analytics. Nonetheless, the reliance on massive medical datasets presents the problems of reliable storage, reliable cooperation, and susceptibility to adversarial interference [13-15]. Current solutions have the disadvantage of being computationally expensive, lacking interoperability, being slow, and lacking robustness to advanced cyberthreats, limiting their use in a real-time healthcare setting.The purpose of this study is to address these concerns.

Novelty and Contribution

The following is a list of the innovations and contributions of this paper:

- A novel preprocessing strategy, Joint Frame-Level and Block-Level Rate-Perception Optimized Preprocessing (JFL-BLRPOP), is introduced to enhance ECG signal perceptual consistency by jointly optimizing temporal frames and block structures, enabling robust noise suppression and improved signal representation.
- An advanced feature extraction mechanism using Synchrosqueezing-based Short-Time Fractional Fourier Transform (S-STFFT) is developed to capture precise time–frequency characteristics of ECG signals, improving discriminative feature learning for complex cardiac pattern analysis under varying signal conditions.
- A deep learning architecture, Parallel Cell Attention 1D Convolutional Network (PCA-1DCN), is designed to model multi-scale temporal dependencies and attention-driven feature refinement, enabling efficient learning of morphological and sequential ECG characteristics for reliable classification performance.
- The Cuckoo Catfish Optimizer (CCO) is incorporated to adaptively optimize network parameters, enhancing convergence behavior and balancing exploration–exploitation processes during training, thereby improving model generalization and stability without manual hyperparameter adjustment.
- A secure healthcare framework employing Holistic Blockchain Consensus Spectral Graph Neural Network (HBC-SGNN) is proposed to ensure trustworthy ECG data management, decentralized validation, and intelligent cyber-attack detection, strengthening cybersecurity and integrity within distributed medical data ecosystems.

This document is organized as follows. There are five major sections in this manuscript. The overview and background are covered in Section 1. The related work and the corresponding methodologies are presented in Section 2. Section 3 describes the suggested methods and their components. The experimental outcomes are summarized and analyzed in Section 4. Section 5 provides a summary of the results and conclusions.

2. Literature Survey

Numerous studies have employed a blockchain-based cybersecurity framework and ECG signal classification. A couple of them are covered in this section.

In 2025,Selvam et al. [16] presented a hybrid deep learning architecture, Convolutional Neural Network-Variational Autoencoder (CNN-VAE), which can automatically classify electrocardiography-based cardiovascular disease.The method is a convolutional feature extraction and latent representation learning method, which is used to detect normal and disease patterns in the 12-lead records of PTB-XL data. The design facilitated the characterization of features of multi-class ECG interpretation, facilitating early diagnosis. The research, however, relied on one dataset, which narrowed the generalization to a wide range of clinical populations.

Yang et al. (2025) [17] presented a research study investigating information fusion of 12-lead electrocardiogram signals to make a cardiovascular diagnosis using artificial intelligence. Correlation among the leads and the multi-label nature were considered by experimenting with various lead combinations and fusion schemes. An artificial brain structure called Lead-5-Group Net (L5G-Net) arranges leads to medical-inspired groups to enhance complementary data use. The method was based on preset lead grouping and was not tested on a variety of clinical data that restricted extrapolation in practice.

In 2025,Liu et al. [18] introduced ECG-STAR Net (Spatio-Temporal Attention Residual Network), a deep learning model to classify multiple electrocardiogram abnormalities (arrhythmias and cardiac diseases) based on multi-label classification. It represented a neural architecture that combined linear layers, a long short-term memory network, spatial-temporal convolutions, and channel attention to consider complicated temporal and

spatial dynamics in ECG signals. The model was tested on several benchmark ECG data to facilitate automated cardiac diagnosis. It was, however, computationally complex.

Borah et al. (2024) [19] presented a Knowledge Distillation-based Convolutional Neural Network (KD-CNN) model to detect and localize Myocardial Infarction using 12-lead ECG data. The approach used ECG data from the PTB-XL dataset and classified major diagnostic classes associated with myocardial infarction. Deep learning was used to interpret cardiac patterns in ECG recordings automatically. Further validation employed a combination of datasets in several hospitals and sources. However, the study found that there were limitations to the application of diversity of datasets and that there were issues of generalization.

In 2024,Kutluanaand Türker [20] demonstrated an electrocardiogram signal classification paper in which time-series ECGs were converted into visibility graphs, and informative diagonals of adjacency matrices were mined as compact features to be analyzed by deep learning. The characteristics were modeled through the Residual Network (ResNet) model to represent structural relations in PTB-XL signals. This method enhanced ECG data feature representation, and adjacency matrix processing reduced preprocessing costs in largedata sets.

Alotaibi(2025) [21] introduced a cybersecurity architecture of IoT-based smart environments involving deep learning, SDN, and blockchain to improve the security of communication, detection of threats, and data robustness. The Squeeze-Excitation based Bidirectional Long Short-Term Memory with Honey Badger Algorithm (SE-BiLSTM-HBA) was used to traffic analyze and detect intrusion, and blockchain was used to handle secure data and transaction management. The imbalance of data during training was resolved by SMOTE. Nonetheless, the architecture made the computations and the number of resources more complex, becoming impractical in the case of lightweight IoT devices.

Kolsur and Hosmani (2025) [22] demonstrated an Artificial Intelligence-driven Healthcare Cybersecurity System (AI-HCSS) that incorporates blockchain technology that can block cyber-attacks on IoT-based healthcare settings. The framework used healthcare data and converted it to a more simplified format with better normalization and entropy-based feature extraction, then identified a DDoS attack with a modified Parallel Convolutional Neural Network. The medical data storage was guaranteed to be irreversible and secure through blockchain, whereas transparency was enhanced through the explainable analysis. Nevertheless, the methodology made it more complex to compute and demanded large resources in order to implement it in real-time.

In 2025,Khan et al. [23] presented a Blockchain Distributed Ledger Technology-Internet of Medical Things (BDLT-IoMT) architecture incorporating a combination of blockchain and machine learning to manage healthcare information securely. The system also resolved the challenge of interoperability since it was able to support decentralized storage, secure data exchange, and smart communication among the heterogeneous IoMT devices and automated decision-making with support of support vector machine models. Another use of blockchain was to transfer and exchange distributed training data and ensure integrity among nodes. Nonetheless, architecture was also associated with the augmented computational load and complexity in large-scale IoMT networks.

Patil et al. (2025) [24] presented a blockchain application to improve security and privacy in smart healthcare big data management. The study introduced the idea of a Blockchain-Based Privacy Preservation Framework (PPF), which is based on blockchain and single public-key cryptography, linked ring signatures on an elliptic curve cryptography system, and secures multiparty computation to safeguard healthcare data and prevent cyber-attacks in decentralized systems.The framework boosted privacy and data security in healthcare settings, but the problem of scalability and increased complexity of the system was still a constraint.A comparison of the current methods is presented in Table 1.

Table 1: A comparison of the current methods

Authors Name	**Methods**	**Advantage**	**Disadvantage**
Selvam et al. [16]	CNN-VAE	The hybrid architecture captured richer ECG signal representations.	Reliance on a single dataset limits cross-population generalization.
Yang et al. [17]	L5G-Net	Uses inter-lead relationships to enhance ECG representation learning	Pre-defined lead grouping may limit adaptability across datasets

Liu et al. [18]	ECG-STAR Net	Captured complex spatial and temporal ECG feature relationships	High model complexity requires greater computational resources
Borah et al. [19]	KD-CNN	Automatic MI detection and localization using deep learning	Performance may vary with different patient datasets
Kutluanaand Türker [20]	ResNet	Extracts structural temporal information using visibility graphs	Visibility graph construction increases computational preprocessing complexity
Alotaibi [21]	SE-BiLSTM-HBA	Accurate and robust detection of diverse IoT cyber threats	High computational overhead and complex implementation
Kolsur and Hosmani [22]	AI-HCSS	Strong protection of healthcare IoT data using blockchain and AI	High computational cost and resource requirements
Khan et al. [23]	BDLT-IoMT	Ensured secure decentralized data sharing and interoperability	High computational overhead and scalability complexity
Patil et al. [24]	PPF	Enhanced privacy protection and secure healthcare data sharing	Scalability limitations and increased system complexity

2.1 Problem Statement and Research Gap

Recent developments of automated electrocardiogram (ECG) classification have made great progress in the diagnosis of cardiovascular diseases, but there are still a number of essential issues. Current methods are very susceptible to noise and inter-patient variability of signals, thus compromising the reliability of classification in a real-world clinical setting. Furthermore, a large number of traditional deep learning models do not provide an effective method of capturing both temporal and spectral features of ECG signals at the same time, which provides incomplete feature representation. The traditional convolutional neural networks are also deficient in the means of modeling parallel attention-based dependencies among various cardiac patterns. Moreover, the general speed of convergence and parameter instability are common in popular optimization algorithms, which constrain the overall performance of a model. Moreover, the majority of current ECG classification models do not consider the aspects of data security and integrity, which are critical to healthcare applications that require sensitive patient data. To overcome these research gaps, the proposed study uses a new framework of PCA-1DCN-CCO that incorporates the elements of robust signal preprocessing, S-STFFT-based time frequency feature extraction, a PCA-1DCN to learn features much better, CCO to tune the parameters, and a blockchain-based module to provide the secure and tamperproof management of ECG data.

3. Proposed Methodology

The suggested framework operates on a guided pipeline of secure and correct ECG classification combined with cybersecurity measures. The initial process involves the ECG signals obtained by the PTB-XL dataset being processed using JFL-BLRPOP, which enhances signal quality through a mutual balanced rate-perception approach, eliminating noise and preserving required cardiac patterns. Subsequently, the refined signals are operating S-STFFT, the procedure of isolating discriminative time-frequency features, extracting the time variations together with the spectral content of the ECG signals.These informative characteristics are then fed to

the PCA-1DCN model, in which parallel cell attention mechanisms acquire multi-scale dependencies and focus on clinically meaningful waveform features in order to effectively classify them. CCO is also used to optimise network parameters automatically, in order to balance between exploration and exploitation during training and to enhance the stability of the model. After classification, the HBC-SGNN provides secure data processing and monitoring of cyber-attacks, and combines the blockchain consensus with spectral graph learning to authorize transactions, identify malicious behaviors, and ensure data integrity. This workflow chain guarantees effective signal processing, smart classification, optimized learning, and safe decentralized control in contemporary healthcare settings.The introduced strategy is depicted in Figure 1.

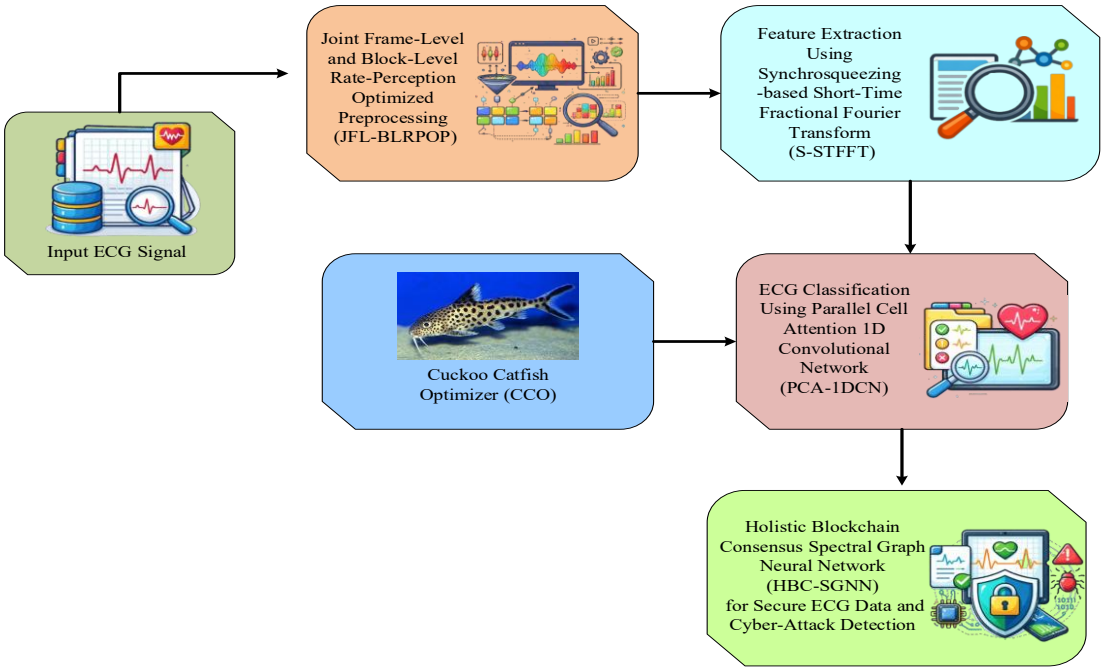


Figure 1: Illustration of the Suggested Methodology

3.1 Input Acquisition

The proposed framework takes ECG signals on the PTB-XL dataset as the input and offers various annotated cardiac recordings, which are reliable to analyze and can be used as the initial step before preprocessing and further processing stages.

3.2 Joint Frame-Level and Block-Level Rate-Perception Optimized Preprocessing (JFL-BLRPOP)

First, the data of the ECG signal, which is retrieved in the PTB-XL Dataset, is preprocessed to enhance the signal quality prior to deep learning classification. Joint Frame-Level and Block-Level Rate-Perception Optimized Preprocessing (JFL-BLRPOP) [25] in the proposed blockchain-based cybersecurity scheme eliminates redundant signal elements and improves clinically significant ECG patterns. This method is a combination of block-level perceptual filtering and frame-level optimization to enhance signal representation.

To find the amount of signal variation that can be removed without changing the important cardiac waveform properties, like the P wave, the QRS complex, and the T wave, the perceptual distortion threshold of ECG signal blocks is computed. This threshold estimation combines perceptual adaptation variables to create the sensitivity of the ECG signal sections.

$$K_F\left(z,d,G,type,M\right)=\Psi\left(M\right)\cdot K_{Base}\left(G_{z,d},G_{0,d},G_{z,0}\right)\cdot G_{LA}\left(G_{z,d},\mu_a\right)\cdot G_{CM}\left(G_{z,d},\mu_f\right)\cdot G_{TY}\left(type,M\right) \quad (1)$$

In Equation (1), $K_F\left(z,d,G,type,M\right)$ represents the perceptual distortion threshold for an ECG signal block used during preprocessing. The parameters z and d denote the frequency indices of the transformed ECG signal coefficients G, while $type$ indicates the structural category of the ECG block and M represents the block size. The normalization factor $\Psi\left(M\right)$ adjusts the threshold based on the block dimension. The term $K_{Base}\left(G_{z,d},G_{0,d},G_{z,0}\right)$ represents the base perceptual threshold derived from spatial contrast sensitivity. The luminance adaptation component $G_{LA}\left(G_{z,d},\mu_a\right)$ models the influence of the mean ECG signal intensity μ_a, whereas the contrast masking factor $G_{CM}\left(G_{z,d},\mu_f\right)$ captures the effect of local signal energy μ_f. Finally,

$G_{TY}\left(type, M\right)$ denotes the block-type adaptation factor that adjusts perceptual sensitivity for different ECG signal patterns.

The perceptually unimportant signal coefficient is eliminated by the smoothing filtering step, and significant ECG information is retained. In the process, redundant noise elements are eliminated, leaving diagnostically important features needed to classify ECGs with high accuracy using deep learning.

$$\hat{G}_{z,d} = \begin{Bmatrix} Sgn\left(G_{z,d}\right)\cdot\sqrt{G_{z,d}^2 - K_F^2\left(z,d\right)} & ,\left|G_{z,d}\right| > K_F\left(z,d\right) \\ 0 & ,Otherwise \end{Bmatrix} \quad (2)$$

In Equation (2), $\hat{G}_{z,d}$ denotes the filtered ECG coefficient obtained after applying the smoothing operation. The variable $G_{z,d}$ represents the original transformed ECG signal coefficient, while $K_F\left(z,d\right)$ corresponds to the perceptual distortion threshold determined previously. The magnitude term $\left|G_{z,d}\right|$ determines whether a coefficient exceeds the perceptual threshold. The function $Sgn\left(G_{z,d}\right)$ preserves the polarity of the ECG coefficient during filtering.When the value of the coefficient exceeds the threshold, the square-root transformation is used to reduce the value; otherwise, the coefficient is set to zero. This is an effective operation to eliminate redundant signal energy, maintaining beneficial ECG waveform characteristics to be analyzed later.

The frame-level optimization step will be used to figure out the optimal preprocessing parameter that balances the perceptual signal quality and efficient representation. This optimization is to make sure that the preprocessing stage optimizes perceptual enhancement and minimizes redundant data in the ECG signal sequence.

$$\omega^* = Arg\max\left\{\Delta SH_{QNXG\sim\alpha}\left(Q,\Phi,\omega\right)\right\} \quad (3)$$

In Equation (3), ω^* represents the optimal preprocessing parameter obtained through an optimization process. The operator $Arg\max$ identifies the value that maximizes the objective function. The term $\Delta SH_{QNXG\sim\alpha}\left(Q,\Phi,\omega\right)$ denotes the perceptual rate-distortion improvement achieved after preprocessing the ECG signal sequence. The variable Q represents the original ECG signals obtained from the PTB-XL dataset, while Φ denotes the set of signal processing parameters associated with the encoding or transformation process. The parameter ω represents the adjustable preprocessing control factor.Using this optimization, the ECG signals are optimized to have better perceptual quality and less redundancy, and the resulting preprocessed ECG data is then sent to the feature extraction stage in the blockchain-based cybersecurity model to classify ECGs using deep learning.

3.3 Feature Extraction Using Synchrosqueezing-based Short-Time Fractional Fourier Transform (S-STFFT)

Preprocessing is followed by feature extraction to extract discriminative representations of ECG signals to be used in deep learning-based classification. The proposed blockchain-based cybersecurity model takes the preprocessed ECG signal of the PTB-XL dataset as data to input Synchrosqueezing-based Short-Time Fractional Fourier Transform (S-STFFT) [26]. The method improves time-frequency energy concentration and exposes non-stationary ECG patterns in the form of P-wave, variability of QRS complex, and morphological variability of T-wave.

The former is the first step that models the ECG signal as an analytic mono-component signal representation on which time-frequency analysis is performed. This representation will record the instant amplitude and phase value of the ECG signal as indicated in Equation (4).

$$d\left(g\right) = X\left(g\right)h^{p\phi(g)} \quad (4)$$

Where $d\left(g\right)$ represents the preprocessed ECG signal. The term $X\left(g\right)$ represents the instantaneous amplitude of the ECG signal. It indicates the strength of the cardiac electrical activity. $\phi\left(g\right)$ represents the instantaneous phase function of the ECG signal. The complex exponential term represents the oscillatory nature of the signal, and p represents the imaginary unit.This complex representation enables the ECG signal to be represented in the time-frequency space to obtain dynamic cardiac information.

The step also includes the calculation of the short-time fractional fourier transform, which is calculated by using the synchrosqueezing to come up with a focused time-fractional representation of the ECG signal in terms of frequencies. This transform produces coefficients that indicate the distribution of energy of the signal both in time and relative frequency, as illustrated in Equation (5).

$$K_{d,\alpha}^{e}\left(g,z\right) = \frac{Y_\alpha\, X\left(g\right)h^{q\phi(g)}}{Y_\beta} E_\beta\left(z\, Sin\,\beta\csc\alpha - \phi'\left(g\right)Sin\,\beta\right) \quad (5)$$

Where $K^{e}_{d,\alpha}(g,z)$ denotes the S-STFFT coefficient representing the time-fractional frequency distribution of the ECG signal. The parameter α represents the fractional transform order controlling the orientation of the time-frequency plane, while g indicates the time variable and z denotes the fractional frequency coordinate. The constant Y_{α} is a normalization factor related to the fractional transform and Y_{β} represents a scaling parameter associated with the transform kernel. The term $E_{\beta}(\cdot)$ corresponds to the β-order fractional Fourier transform of the window function. The derivative $\phi'(g)$ indicates the instantaneous frequency of the ECG signal. For the purpose of feature extraction, this transformation offers a condensed and focused representation of the ECG signal.

The last procedure is synchrosqueezing to reallocate the time-frequency energy along the instantaneous frequency path of the ECG signal. A more focused representation of the signal energy is obtained in this reassignment process, as represented in Equation (6).

$$GK^{e}_{d,\hat{\alpha}}(g,\eta)=\int_{R} K^{e}_{d,\hat{\alpha}}(g,z)\delta\left(\eta-\hat{z}_{\hat{\alpha}}(g,z)\right)dz \tag{6}$$

Where $GK^{e}_{d,\hat{\alpha}}(g,\eta)$ represents the synchrosqueezed time-fractional frequency energy distribution of the ECG signals. The variable η denotes the reassigned fractional frequency coordinate where the energy is concentrated. The term $K^{e}_{d,\hat{\alpha}}(g,z)$ represents the original S-STFFT coefficients before reassignment, and z indicates the original fractional frequency coordinate. The function $\hat{z}_{\hat{\alpha}}(g,z)$ denotes the instantaneous fractional frequency estimator derived from the transform coefficients. The symbol $\delta(\cdot)$ represents the Dirac delta function, which relocates the energy to its correct frequency position.

In the process, the time-frequency representation is concentrated to a large extent, facilitating the derivation of discriminative ECG features of the deep learning-based classification model.

3.4 ECG Classification Using Parallel Cell Attention 1D Convolutional Network (PCA-1DCN)

The study aims to create an effective ECG classification model with a Parallel Cell Attention 1D Convolutional Network (PCA-1DCN). It is a hybrid design that combines Cell Attention Networks (CANs) [27] and Parallel 1D-Convolution (P-1D-C) [28] to discover discriminative patterns of ECG signals. The input of ECG classification is the extracted features that allow for detecting the cardiac abnormalities correctly.

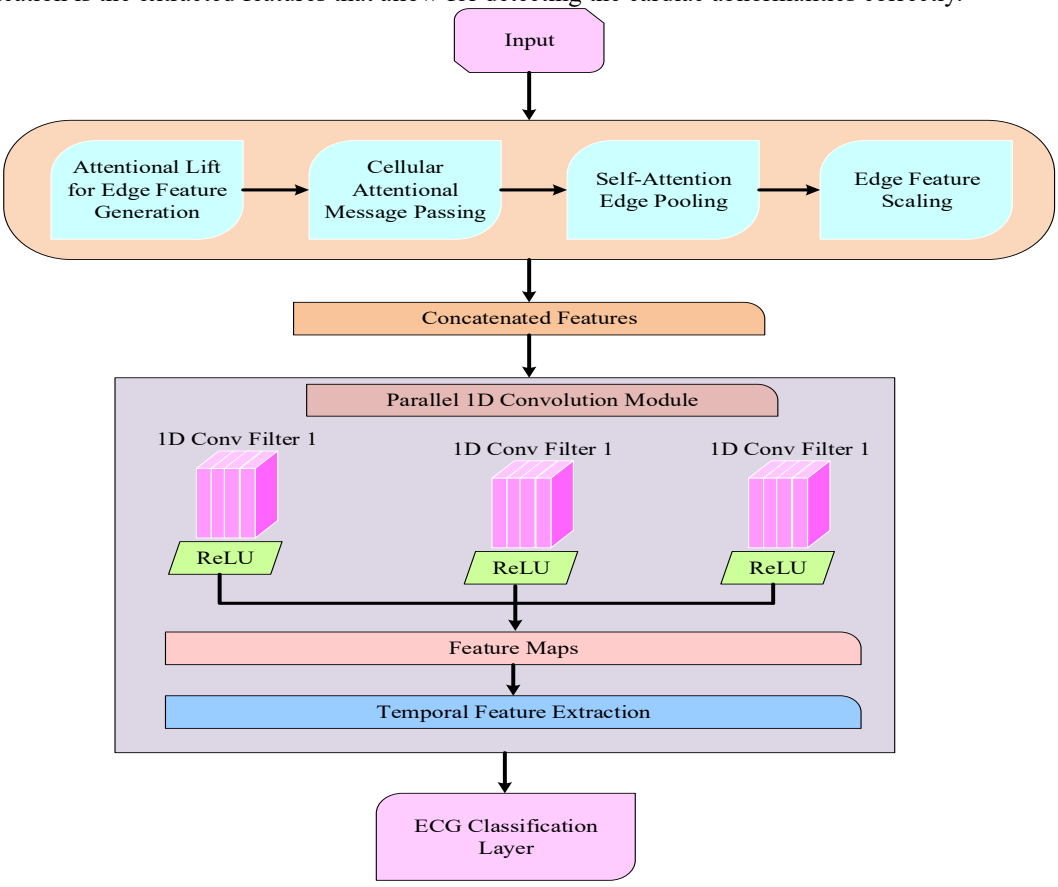


Figure 2: Architecture of PCA-1DCN

Figure 2 shows the structure of the parallel cell attention 1D convolutional network (PCA-1DCN) model for ECG classification. The input signal is passed through edge feature enhancement using attentional lift, cellular message passing, self-attention pooling, and feature scaling. The features are concatenated and passed through a parallel 1D convolutional layer with multiple filters and ReLU activation functions to extract features from the input signal. The ECG classification layer is responsible for classifying the ECG signal and includes spatial and temporal patterns of ECG signals.

- **Attentional Lift for Edge Feature Generation**

Cell Attention Networks convert graph-structured representations of ECGs into higher-order cell complexes to learn complicated dependencies among cardiac signal segments. The proposed PCA-1DCN model will map extracted features of the ECG into node representations and lift them into edge-level features at the first stage, using an attentional mechanism. Attentional lift calculates edge features between pairs of nodes linked by an edge based on a multi-head attention. This operation enables the model to obtain relations among ECG signal parts, including P-wave, QRS complex, and T-wave, as presented in Equation (7).

$$p_g = e\left(p_a, p_b\right) = \Big\|_{s=1}^{L^0} x_m^s\left(p_a, p_b\right), \qquad \forall g \in \varepsilon \tag{7}$$

Where p_g is the generated edge feature vector used for the classification of the ECG. The function $e(\cdot)$ signifies the application of the attentional lift function to map node features to edge features. The variables p_a and p_b signify the feature vectors of the nodes a and b, respectively, generated from the ECG signal segments. The parameter L^0 signifies the number of attention heads used to calculate multiple attention scores. The function $x_m^s(\cdot)$ signifies the $s-th$ learnable function used to calculate the importance of each pair of nodes. The symbol $\|$ signifies the concatenation operator used to combine the output of each attention head to obtain the final edge feature vector.

- **Cellular Attentional Message Passing**

Following the edge representation generation, the PCA-1DCN model passes attentional messages to cells to update edge embeddings based on upper and lower adjacency relations in the cell complex representation of ECG signals. The edge embedding update is based on the information about neighboring edges that share similar nodes or are located in the same polygonal cell structure. The update process allows the effective modeling of spatial dependencies in ECG signal graphs as defined in Equation (8).

$$\widetilde{u}_g^v = \phi^v\left(u_g^v, \bigoplus_{s \in M_k^v(g)} x_k^v\left(u_g^v, u_s^v\right)\psi_k^v\left(u_s^v\right), \bigoplus_{s \in M_f^v(g)} x_f^v\left(u_g^v, u_s^v\right)\psi_f^v\left(u_s^v\right)\right) \in R^{L^{v+1}} \tag{8}$$

Where $\widetilde{u}_g^v$ represents the updated edge embedding for ECG feature representation. The vector u_g^v represents the previous layer edge feature representation. The function $\phi^v(\cdot)$ represents the learnable transformation applied to the aggregated messages. The sets $M_k^v(g)$ and $M_f^v(g)$ represent the lower and upper neighboring edges associated with the edge g. The attention functions $x_k^v(\cdot)$ and $x_f^v(\cdot)$ calculates the importance between edges that share the node or are part of the same polygon. The functions $\psi_k^v(\cdot)$ and $\psi_f^v(\cdot)$ represent the learnable transformations applied on the neighboring edge embeddings.

- **Self-Attention Edge Pooling**

In order to minimize the computational complexity and select the most informative ECG relationships, a self-attention edge pooling mechanism is used after each message-passing layer in the CAN component. The pooling mechanism computes a self-attention score of all features of an edge and then chooses the most important ones to be extended as specified in Equation (9).

$$\gamma_g^v = x_i^v\left(\widetilde{u}_g^v\right) \qquad \forall_g \in \varepsilon^v \tag{9}$$

Where γ_g^v is the attention pooling score for the edge g. The function $x_i^v(\cdot)$ is a learnable pooling attention function that measures the importance of the edge embeddings. The variable $\widetilde{u}_g^v$ represents the edge feature vector that is computed after the message passing stage. The attention scores will define the edges to be included in the cell complex representation for ECG classification.

- **Edge Feature Scaling After Pooling**

Once the most significant edges are selected, those features that were retained are scaled based on the attention scores that they obtained to maintain their relevance to the ECG classification pipeline. In this scaling operation, edges that are more important in the resultant representation dominate more in the learned representation as defined in Equation (10).

$$u_g^{v+1} = \gamma_g^v \, \widetilde{u}_g^v \qquad \forall_g \in \varepsilon^{v+1} \tag{10}$$

Here, u_g^{v+1} represents the updated edge feature vector after the pooling operation. The parameter γ_g^v indicates the self-attention score for the edge g. The vector $\widetilde{u}_g^v$ represents the original edge embedding vector before the pooling operation. The scaling mechanism is used to highlight the most significant ECG signal relationships in the proposed PCA-1DCN architecture.

- **Parallel 1D Convolution Feature Extraction**

After the cell attention processing, the learned ECG representations are sent to the parallel 1D convolution module. This module combines three ECG feature streams in parallel to ensure that it gets the temporal dependencies of the signal. The features of every convolution channel are obtained in a given ECG input stream through a set of trainable filters and activation functions, as defined in Equation (11).

$$z^d = \left[z_1^d, z_2^d, ..., z_L^d \right] \in R^{G \times L} \tag{11}$$

Where z^d represents the output feature map of the $d-th$ convolution channel. The vector components z_b^d represent the output of the $b-th$ convolution filter. The parameter G represents the total number of convolution filters used in the parallel convolution layer. The feature maps contain the necessary temporal patterns of the ECG signals for classification.

- **Convolution Operation for ECG Feature Learning**

The parallel convolution layer includes the convolution operation and nonlinear activation in every filter that learns the discriminative patterns of ECG signals. The computation of the convolution of every filter is given in Equation (12).

$$z_b^d = \ell\left(\widetilde{p}^d * s_b^d + y_b^d \right) \in R^{G \times 1} \tag{12}$$

Here, z_b^d represents the feature output obtained from the $b-th$ convolution filter applied in the $d-th$ stream. The function $g(\cdot)$ represents the ReLU activation function that is applied to introduce nonlinearity in the model. The vector $\widetilde{p}^d$ represents the normalized input ECG signal. The parameter s_b^d represents the convolution kernel that is learned for extracting ECG features. The variable y_b^d represents the bias applied to the convolution filter.

The input to the ECG classification layer in the proposed PCA-1DCN is the concatenated features obtained from the CAN and P-1D-C modules. The discriminative representations learnt by the classifier are used to identify abnormal ECG patterns to ensure secure healthcare monitoring in the cybersecurity model based on blockchain. Lastly, the Cuckoo Catfish Optimizer(CCO) is used to optimize key hyperparameters of the PCA-1DCN model, to enhance the performance of the model in terms of classification accuracy and stability.

3.5 Cuckoo Catfish Optimizer (CCO)

The Cuckoo Catfish Optimizer (CCO) [29] is based on the reproductive behavior of the cuckoo catfish (Synodontismultipunctatus in Lake Tanganyika), which is a parasite. This fish uses the host cichlids to raise its young ones by inserting its eggs inside the eggs of the host. A number of biological behaviors that CCO models include adaptive movement toward supportive environments, invasion of host nests by groups, and competition among offspring. All those behaviors can be modeled with the help of such strategies as circling search, compressed space exploration, chaotic predation, and regeneration mechanisms to allow the algorithm to balance exploration and exploitation efficiently in the course of optimization.Figure 3 shows the methodical process of CCO.

Step 1: Initialization

Once the parameters of the CCO method are chosen, the optimization process starts. Once the optimization environment is set up, PCA-1DCN can effectively and consistently reduce the bias parameter.

Step 2: Random generation

The search starts with a random selection of possible answers. To keep solutions from converging, variability can be controlled at the random generating stage. The responses point to a possible bias parameter in PCA-1DCN. CCO iteratively refines the random choices to generate the optimal options.

Step 3: Fitness Function

In this way, the fitness function uses the existing bias to assess the performance quality of the PCA-1DCN candidate solution. Equation (13) provides the fitness function to evaluate the quality of the solution and provide performance feedback to guide optimization by varying the bias value.

$$Fitness \;\; Function = Min\left(y \right) \tag{13}$$

Where y indicates PCA-1DCN's bias parameter.

Step 4: Exploration Phase

The exploration stage of the Cuckoo Catfish Optimizer (CCO) is aimed at scanning the global solution space to identify good areas. This step approximates the adaptive behavior of cuckoo catfish as it moves and searches in

groups. Compressed space search and surround search are some of these strategies that allow the population to be diversified and avoid convergence.

$$P_x^{New} = P_x + U_1 \times \left|\ell s\right| \times \left(\frac{P_{Best} + P_{\ell 1}}{2} - P_{\ell 2} \right) + \frac{\ell_3}{2} \times \left(P_{\ell 3} - P_{\ell 4} \right) \quad (14)$$

The update of the positions in the exploration phase is done using Equation (14), where P_x^{New} represents the updated positions for the $x-th$ cuckoo catfish individual, and P_x represents the current positions of the individual in the search space. P_{Best} represents the global best solution, which is the prey position. $P_{\ell 1}, P_{\ell 2}, P_{\ell 3}$ and $P_{\ell 4}$ are random individuals from the population that introduce diversity in the search process. U_1 is a random binary variable that determines the feasibility of the movement, ℓs is the intensity of the cooperative interaction that is normally distributed, and ℓ_3 is the random number for the adjustment of the exploration movement.

Step 5: Exploitation Phase

The Cuckoo Catfish Optimizer exploitation phase focuses on optimizing solutions around good regions that have been identified in the course of exploration. At this level, people focus on vigorous searching towards the optimal ones, emulating the predatory nature of the cuckoo catfish that is approaching cichlid nests. This mechanism increases the accuracy of the solution and the convergence rate towards the optimum solution.

$$P_x^{New} = \begin{cases} P_{Best} + K \times G \times \left(P_{Best} - P_x \right) & If\ Y_x > Y_{In} \\ P_{Best} \times \left(1 + L^5 \times Z_q \times O \right) + K \times G \times \left(P_{Best} - P_x \right) & Else\ If\ Y_x > Y_{In} \times V_p \\ P_{Best} \times \left(1 + L^5 \times H_e \right) + K \times G \times \left(P_{Best} - P_x \right) & Otherwise \end{cases} \quad (15)$$

The exploitation stage involves the updating of the search position based on the predation behavior represented in Equation (15). Here, P_x^{New} represents the updated position of the $x-th$ individual, whereas the current position of the individual is represented by P_x. The best solution obtained so far is represented by P_{Best}. The direction factor K takes the value of either -1 or 1, whereas the step scaling factor G represents the movement of the individual. The aggregation degree of the current individual is represented by Y_x, whereas the initial population aggregation degree is represented by Y_{In}. The warning factor is represented by V_p, the shrinkage factor is represented by L, the chaotic coefficient for small prey movement is represented by Z_q, the kinetic energy factor is represented by O, and the Gaussian chaotic coefficient for large prey movement is represented by H_e.

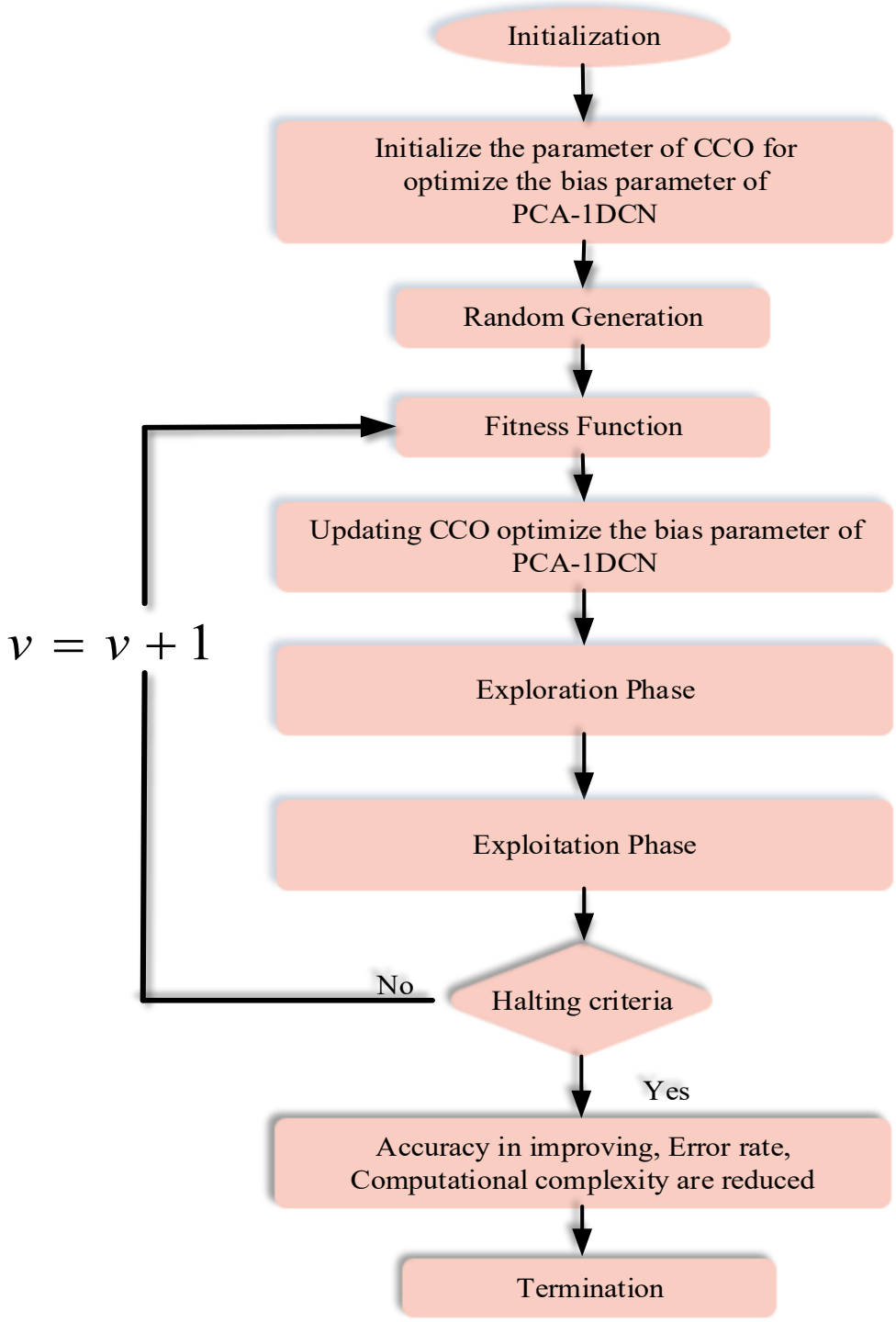


Figure 3: Step-by-step procedure of CCO

Step 6: Termination

When the optimization process reaches the termination phase and meets the requirements for termination, it is considered complete. At this termination point, the CCO method effectively lowers the bias parameter of the PCA-1DCN. Even with the current benefits of convergence, further modification would not yield noticeable gains in performance. Model convergence demonstrates that optimization is finished before performance improvements are insignificant or impossible.

3.6 Holistic Blockchain Consensus Spectral Graph Neural Network (HBC-SGNN) for Secure ECG Data and Cyber-Attack Detection

During this stage, the ECG signals attained in the ECG classification stage are classified according to their significance as the input into the cybersecurity framework. The proposed Holistic Blockchain Consensus Spectral Graph Neural Network (HBC-SGNN) incorporates Holistic Blockchain Consensus verification [30] as a strategy to achieve secure ECG storing and transmission, and Spectral Invariant Graph Neural Networks

(SIGNN) [31] study as a method to identify cyber-attacks through analysis of patterns in the structure of blockchain communication.

- **Blockchain Consensus Message Validation**

The Holistic Blockchain Consensus system is used to determine the authenticity of ECG transaction messages being relayed through the blockchain network. Equation (16) means that the blockchain state variable grows with every validated ECG transaction that is broadcast by a correct node.

$$y_0^{New} = y_0 + 1 \tag{16}$$

Here, y_0^{New} represents the updated number of verified ECG broadcast messages recorded in the blockchain. The variable y_0 represents the current number of broadcast messages sent by correct nodes.The successful validation and propagation of a new ECG transaction in the distributed blockchain network is represented by the increment operation.

- **Byzantine Fault-Tolerant Broadcast Threshold**

The consensus protocol checks the number of confirmations that a broadcast message has been sent to network nodes. The validity of a broadcast ECG transaction is defined as the number of received messages surpassing the Byzantine threshold according to Equation (17).

$$y_1 \geq f + 1 - g \tag{17}$$

The variable y_1 represents the number of broadcast messages received from correct nodes. The parameter f represents the consensus threshold of the nodes that participate in the network. The parameter g represents the maximum number of Byzantine nodes.In the case that this inequality exists, then the blockchain network approves that the ECG transaction is issued by trusted parties.

- **Blockchain Fairness and Iteration Control**

The fairness mechanism makes sure that there is a balanced advancement in blockchain consensus over iterations. As demonstrated in Equation (18), the control factor also declines with the number of consensus iterations.

$$Z = 1 - \frac{It}{MaxIt} \tag{18}$$

The variable Z refers to a consensus adjustment factor that is constantly decreasing. The variable It refers to the iteration number in the verification process of consensus. The variable $MaxIt$ refers to the maximum iteration of consensus. The larger the iteration, the smaller the value of Z, facilitating the transition of the blockchain network from exploration to verification.

- **Blockchain Consensus Termination Condition**

The termination condition ensures that all correct nodes ultimately obtain a validated value on an ECG transaction. In Equation (19), the blockchain consensus mechanism is completed once each node is in the final consensus state.

$$\Diamond\left(\kappa\left[S_0\right] = 0 \wedge \kappa\left[S_1\right] = 0 \wedge \kappa\left[Y_0\right] = 0 \wedge \kappa\left[Y_1\right] = 0 \wedge \kappa\left[Y_{01}\right] = 0\right) \tag{19}$$

The operator $\Diamond$ signifies the eventual convergence of the system state. The function $\kappa\left[\cdot\right]$refers to the number of nodes that exist in a given blockchain state. The variables S_0 and S_1 represent the initial blockchain node states for binary transactions. The states Y_0, Y_1, and Y_{01} represent the intermediate states for the broadcast process.Upon attainment of zero values of these states, all nodes converge to final consensus states, which guarantees safe consensus on ECG transaction data.

- **Spectral Invariant Graph Neural Network for Cyber-Attack Detection**

Once ECG data is secured via blockchain consensus, the Spectral Invariant Graph Neural Network analyzes the communication graph of the blockchain to identify a cyber-attack. Equation (20) states that the spectral tensor representation converts graph spectral quantities in the presence of permutation symmetries.

$$\left[(\sigma,\tau)\cdot A\right]_{p,d,v,q} = A_{\sigma^{-1}(p),\tau^{-1}(d),\tau^{-1}(v),q} \tag{20}$$

The tensor A retains spectral information about the blockchain communication graph. The index p is used to denote the eigenvalue index of spectral components of the graph. The indices d and v denote positions of nodes in the graph. The index q is used to denote the spectral feature dimension. The permutation operators σ and τ are symmetric group elements.This transformation guarantees the neural network to be immune to structural variations in the communication graph and to detect abnormal patterns induced by cyber-attacks.

The suggested framework classifies ECGs securely using a sequence of processing pipelines. JFL-BLRPOP improves the quality of the signal used by minimizing noise and retaining significant cardiac attributes. S-STFFT is an informative time-frequency feature extractor that is learnt by PCA-1DCN to acquire meaningful ECG patterns. CCO maximizes network characteristics and increases training efficiency and stability. Lastly,

HBC-SGNN guarantees safe data management and cyber-attack identification, which occurs on the basis of blockchain-based verification, which allows reliable and scalable as well as trustworthy healthcare data analysis.

4. Results and Discussion

The suggested framework measures the ECG classification and blockchain performance based on detailed metrics like F1 score, recall, specificity, precision, accuracy, error rate, and computational time. Moreover, blockchain performance is evaluated on the basis of latency, throughput, and security level, which allows measuring model reliability, scalability, responsiveness, and secure data management in the deployed Python-based blockchain-integrated system.Table 2 shows the implementation requirements of the proposed model.

Table 2: Implementation Requirements of the Proposed Model

Category	Specification
Dataset	PTB-XL Dataset
Programming Language	Python 3.10
Operating System	Windows 11
Processor	Intel Core i7 Processor
Memory (RAM)	16 GB RAM
Graphics Processing Unit	NVIDIA GeForce RTX 3060
Deep Learning Framework	TensorFlow
Signal Processing Library	NumPy
Training Network	Parallel Cell Attention 1D Convolutional Network (PCA-1DCN)
Optimization	Cuckoo Catfish Optimizer (CCO)

4.1 Dataset Description

The proposed method makes use of the PTB-XL dataset [32] to classify ECG signals and the CICDDoS2019 dataset [33] to detect cyberattacks. Each dataset is explained thoroughly below.

- **PTB-XL Dataset**

The PTB-XL dataset is a large-scale clinical ECG database created to assess state-of-the-art medical signal analysis methods. 21,837 12-lead ECG records from 18,885 people make up the collection. Ten seconds of data at sampling frequencies of 500 Hz and 100 Hz with a resolution of 16 bits made up each ECG record. Gender-wise, the study is well-balanced (52% male, 48% female), and participants' ages range widely (from 2 to 95 years old). According to the SCP-ECG standards, each ECG was labeled with one or more of the 23 subclasses that were divided into five primary groups, comprising both normal and pathological circumstances. ECGs that were unclassified, rare subclasses with less than 20 occurrences in the participant data, and ECGs with a low classification probability for classifying conditions were eliminated from the research study. The 100 Hz sampling frequency was chosen for these operations, and 17,232 ECGs were included in the final dataset.A training set with 80% of the data and a testing set with the remaining 20% make up the dataset. The PTB-XL ECG record distribution per diagnostic class is shown in Table 3.

Table 3: Distribution of PTB-XL ECG Records across Diagnostic Classes

Class Code	Class Description	Number of Records
CD	Conduction Disturbance	3,232
HYP	Hypertrophy	815
MI	Myocardial Infarction	2,936
NORM	Normal ECG	7,185
STTC	ST/T Segment Changes	3,064

- **CICDDoS2019 Dataset**

In this work, CICDDoS2019 was used to implement the models, which include a broad scope of DDoS attacks created by application-layer protocols via both connectionless and connection-oriented communication protocols, including TCP and UDP. There are two broad categories of attacks present in the dataset, namely: reflection-based attacks and exploitation-based attacks. The data obtained are grouped into eighteen classes to be able to train and test effectively. These are the types of attacks, namely Benign, DrDoS_DNS, DrDoS_LDAP, DrDoS_MSSQL, DrDoS_NetBIOS, DrDoS_NTP, DrDoS_SNMP, DrDoS_UDP, LDAP, MSSQL, NetBIOS, Portmap, SYN, TFTP, and UDP. The training dataset has each type of DDoS attack as a separate file, as shown in Table 4. To train the proposed framework on the detection of cyber-attacks, the attack dataset is considered,

where the model is trained to acquire malicious traffic patterns, recognizing the security threat in the blockchain-based healthcare setting.

Table 4: Training and Testing Instances of the CICDDoS2019 Dataset

Training Instances	87,619,771
Testing Instances	3,756,200

4.2 Evaluation Metrics

In order to assess the effectiveness and reliability of the suggested blockchain-based cybersecurity model as a deep-learning ECG classification, a number of performance indicators are used. Accuracy is used to measure the overall prediction accuracy, whilst recall is used to detect true cardiac abnormalities. Precision and F1-score measure the balance of classification, and specificity measures the detection of correct normal signals. Efficiency is measured by computational time, and responsiveness, scalability, and security level of the system are measured by latency, throughput, and the level of security of healthcare data.

Table 5: Metrics of evaluation and equation

Metrics	Formula
Accuracy	$Acc = \frac{T^P + T^N}{T^P + T^N + F^P + F^N}$
Precision	$\Pr e = \frac{T^P}{T^P + F^P}$
Recall	$\mathrm{Re}\, c = \frac{T^P}{T^P + F^N}$
F1-Score	$F1 = \frac{2 * \Pr e * \mathrm{Re}\, c}{\Pr e + \mathrm{Re}\, c}$
Specificity	$Spec = \frac{T^N}{T^N + F^P}$
Latency	$Latency = \frac{\text{Total time taken}}{\text{Number of inferences}}$
Throughput	$Throughput = \frac{\text{Number of inferences}}{\text{Total time taken}}$

The equation and performance measures are displayed in Table 5. Where T^P denotes the true positive, F^P represents the false positive, T^N denotes the true negative, and F^N represents the false negative.

4.3 Performance Analysis

An evaluation of the performance of the PCA-1DCN-CCOis examined here:

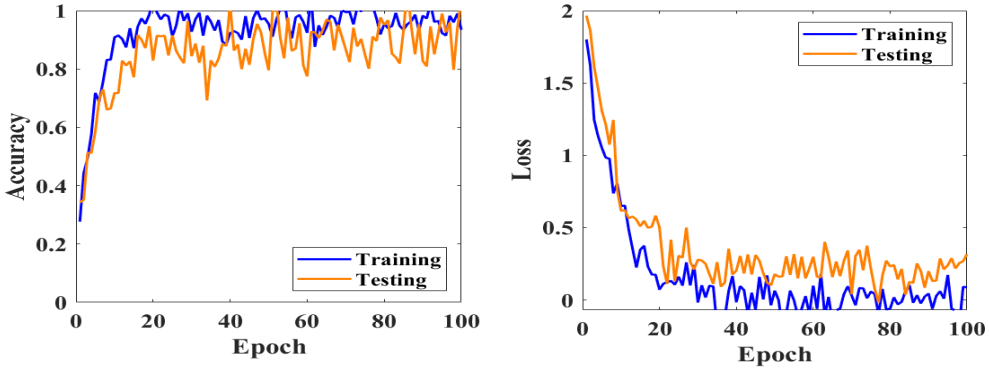


Figure 4: Training and testing accuracy and loss convergence curves across epochs

Figure 4 shows training and testing results of the proposed framework in terms of the accuracy and loss convergence curves versus epoch. The trend of the accuracy improvement and the reduction in the loss are indications that the learning behavior is stable after the preprocessing with JFL-BLRPOP and discriminatory feature extraction with S-STFFT. The PCA-1DCN model is effective in acquiring ECG time-related patterns, but CCO reduces the parameters so as to accelerate convergence and reduce overfitting. The close correlation between the training and testing curve means that the generalization is high. The action confirms that the proposed blockchain-related ECG classification framework has reached stable learning reliability before safe implementation with HBC-SGNN.

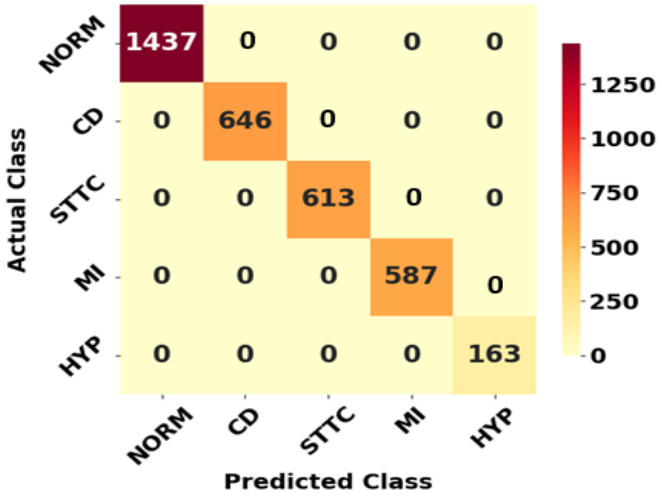


Figure 5: Confusion matrix representing multi-class ECG classification performance

Figure 5 shows the confusion matrix of ECG classification performance under different cardiac classes. The prevalence of the diagonal values shows the correct prediction of the classes due to the improved preprocessing with the application of JFL-BLRPOP and informative time-frequency characteristics obtained with the help of S-STFFT. The attention system of PCA-1DCN captures important ECG waveform features, whereas CCO enhances classification stability by means of optimal parameter estimates. Misclassification is kept to a minimum, which is a good feature of discrimination and learning balance. The accurate identification of classes will aid in confident clinical decision-making, in which the outcomes of classifications are further ensured and verified with the help of the blockchain-based HBC-SGNN cybersecurity system.

Table 6: Class-Wise Performance Evaluation of ECG Classification

Class	Accuracy (%)	Precision (%)	Recall (%)	Specificity (%)	F1-Score (%)
CD	99.68	99.62	99.55	99.60	99.58
HYP	99.72	99.66	99.59	99.63	99.62
MI	99.76	99.71	99.64	99.67	99.67
NORM	99.81	99.78	99.72	99.74	99.75
STTC	99.70	99.65	99.57	99.61	99.61

In Table 6, the performance analysis of the proposed ECG classification model in terms of the classes of CD, HYP, MI, NORM, and STTC is provided by class. The highest performance is demonstrated by the NORM class with the accuracy of 99.81%, the precision of 99.78%, the recall of 99.72%, the specificity of 99.74%, and the F1-score of 99.75%, which means that the pattern is well recognized. MI class has the best accuracy of 99.76% and an F1-score of 99.67%, indicating successful detection of abnormalities. The accuracy of HYP and CD classes is 99.72% and 99.68%, respectively, with balanced metric values. The accuracy and F1-score of STTC are steady and precise with the result of 99.70% and 99.61% respectively, meaning that all the types of cardiac diseases are categorized consistently and at an excellent percentage and F1-score.

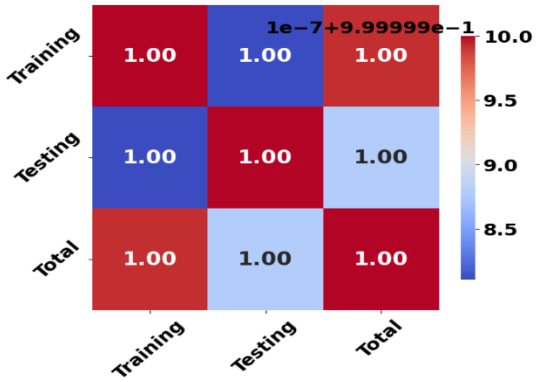


Figure 6: Correlation heatmap showing relationships between training, testing, and overall performance metrics

Figure 6 presents the correlation heatmap between the training, testing, and total performance metrics. Strong correlation means consistency in learning and the ability to predict the proposed methodology. JFL-BLRPOP signal enhancement and spectral feature extraction with the use of S-STFFT generate stable representations, which allow PCA-1DCN to learn the generalized ECG patterns. The parameter tuning by CCO ensures equilibrium optimization among datasets. The homogeneous values of correlation ensure strength and lower levels of variance of performance. This stability is crucial to safe healthcare analytics, in which reliable results are guaranteed prior to blockchain validation and cyber-attack monitoring with HBC-SGNN.

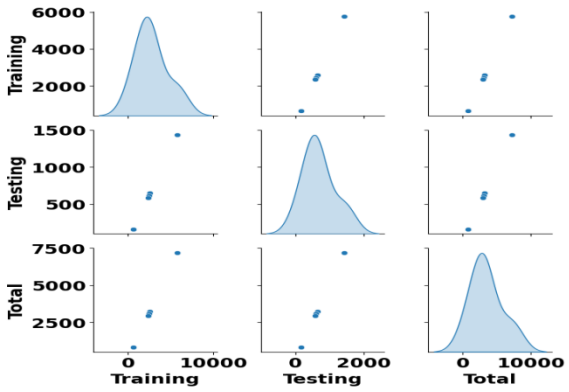


Figure 7: Pairwise distribution analysis of training, testing, and total dataset statistics

Figure 7 shows the statistical relationship between training, testing, and total record distribution as a pair-wise with the help of a density plot and scatter plot. The small clustering effect indicates a homogeneous data distribution obtained through the preprocessing using JFL-BLRPOP that eliminates noise and the morphology of ECG. The compactness of features, which are achieved using S-STFFT, gives the method of separability that allows learning stable feature embeddings using PCA-1DCN. The CCO-based optimization also enables further learning dynamics balance within the datasets. The monotonic statistical framework suggests a lower variance and a stronger model and validates the robustness of the model, which results in stable ECG classification results combined with security monitoring via HBC-SGNN using blockchain.

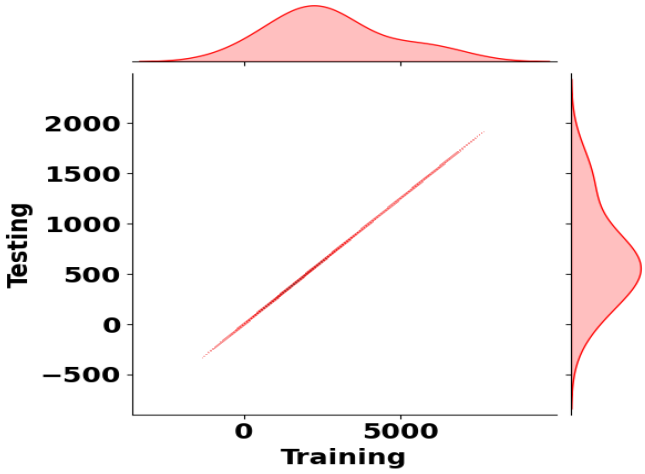


Figure 8: Regression and density analysis showing training data distribution behavior

Figure 8 illustrates the correlation between the training sample and the evaluation distribution using regression and visualization of densities. The linear trend indicates proportional growth of learning attained by the proposed pipeline. PCA-1DCN can learn stable feature mappings on noise-reduced signals as obtained by JFL-BLRPOP and high-resolution representations as obtained by S-STFFT. The CCO optimization balances the model updates to avoid divergence in training. The regular distribution of the density indicates the balanced use of data and the augmented stability of prediction. These features guarantee reliable classification results usable in the blockchain-based HBC-SGNN cybersecurity setting with high levels of reliability in the transmission and verification of results.

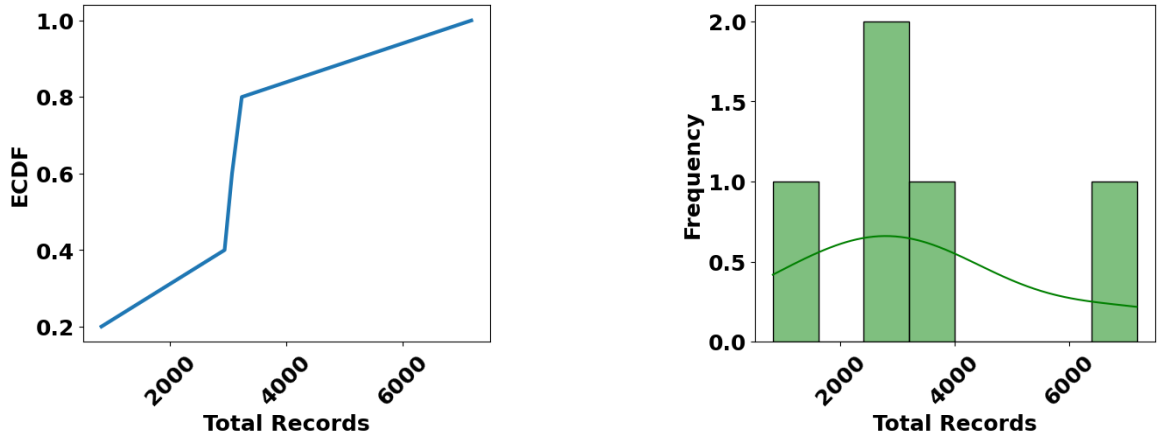


Figure 9: Distribution analysis of ECG records: (a) empirical cumulative distribution function and (b) frequency histogram with density estimation

Figure 9 is a distribution analysis of processed ECG records with two subfigures. Figure 9(a) presents the Empirical Cumulative Distribution Function (ECDF), which depicts the cumulative use of records and progressive coverage of data in the analysis. Figure 9(b) shows the density estimated frequency histogram, which is the distribution of total ECG records. The preprocessing stage guarantees similarity in signal quality, whereas feature learning provides similarity in sample representation. Streamlined classification will guarantee a standardized administration of volumes of records. The balanced patterns of distribution are proven to be scalable and reliable, which can be employed to ensure a safe storage of healthcare data and observability as part of the integrated cybersecurity.

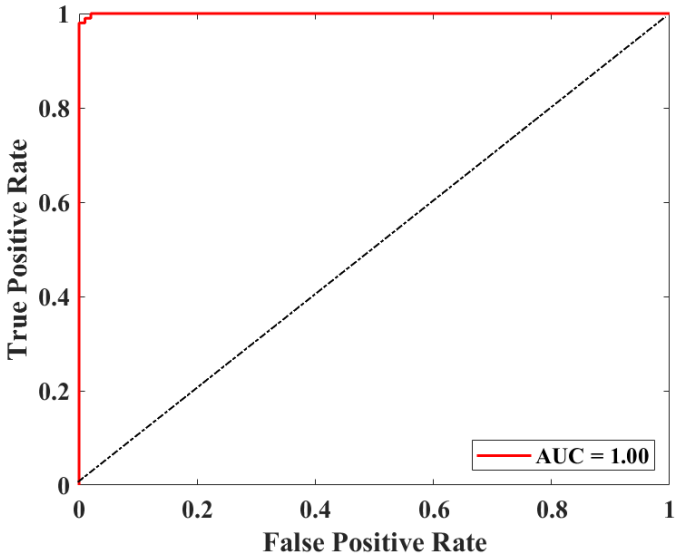


Figure 10: Receiver Operating Characteristic curve demonstrating classification performance

Figure 10 indicates the Receiver Operating Characteristic (ROC) curve that indicates the classification potential of the proposed ECG analysis framework. The trend curve that has been shifting towards the upper left with the value of 1.00 on the AUC indicates high rates of cardiac classes discrimination. Decision boundaries can be optimized through classification through the use of informative feature learning and effective signal enhancement, which will result in proper ECG pattern recognition. Sensitivity is enhanced, and false predictions

are reduced in the preprocessing phase, feature extraction phase, and attention-based learning phases.The trustworthy classification result facilitates secure healthcare analytics, which allows valid downstream blockchain validation and safeguarded medical data management under the unified cybersecurity framework.

4.4 Comparative Analysis

In this section, the performance of the suggested framework will be compared to the performance of various existing methods to classify ECG signals and assess cybersecurity through blockchain. To classify the ECGs based on the PTB-XL dataset, the proposed approach is compared with CNN-VAE [16], L5G-Net [17], ECG-STAR Net [18], KD-CNN [19], and ResNet [20]. Moreover, blockchain performance is compared to SE-BiLSTM-HBA [21], AI-HCSS [22], BDLT-IoMT [23], and PPF [24]. They are compared based on key performance measures such as recall, precision, specificity, F1 score, accuracy, latency, throughput, and computational efficiency to holistically evaluate detection ability, scalability, and effective management of healthcare data with respect to security.

Table 7: Performance Comparison of ECG Classification Methods Using the PTB-XL Dataset

Methods	Acc (%)	Pre (%)	Recall (%)	F1-score (%)	Spec (%)
CNN-VAE [16]	89.55	89.72	89.60	89.66	89.80
L5G-Net [17]	90.18	90.05	90.22	90.13	90.30
ECG-STARNet [18]	90.96	91.02	90.88	90.95	91.10
KD-CNN [19]	91.64	91.50	91.72	91.61	91.80
ResNet [20]	92.31	92.15	92.28	92.21	92.40
PCA-1DCN-CCO (Proposed)	99.71	99.64	99.57	99.60	99.59

Table 7 shows the comparative performance analysis of the proposed PCA-1DCN-CCO framework to the current ECG classification techniques trained on the PTB-XL dataset. The comparison is carried out by the accuracy, precision, recall, F1-score, and specificity measures. The performance values of the existing methods are between 89.55% and 92.31%, reflecting the moderate classification ability. On the contrary, the suggested framework attains much better outcomes in all assessment metrics, providing a better learning of features, the optimization of parameter tuning, and a better consistency of decisions. The high performance validates the framework in the correct detection of cardiac abnormalities and the reliable and robust classification of ECG signals, which can be used to develop intelligent healthcare applications.

Table 8: Error Rate and Computational Time Comparison of ECG Classification Methods

Methods	Error Rate (%)	Computational Time (s)
CNN-VAE [16]	1.21	0.85
L5G-Net [17]	1.08	0.73
ECG-STARNet [18]	0.96	0.64
KD-CNN [19]	0.82	0.52
ResNet [20]	0.69	0.41
PCA-1DCN-CCO (Proposed)	0.01	0.02

Table 8 shows the comparison of the error rate and computer time of existing ECG classification methods and the proposed PCA-1DCN-CCO framework. The existing methods have a greater error rate of 1.21-0.69% and a longer computation time due to inefficient learning and optimization processes. On the other hand, the proposed model has a significantly smaller error rate of 0.01% and a minimum amount of 0.02 seconds of calculation time. Such improvements are indications of a better learning efficiency, convergence, and processing complexity.The findings indicate that the proposed framework presents a precise, time-saving, and dependable ECG classification that can be used in real-time healthcare implementation.

Table 9: Comparative Analysis of Optimization Algorithms for Model Performance Enhancement

Optimizer	Convergence Rate	Iterations to Converge	Computational Time (s)	Memory Usage (MB)	Accuracy (%)
Adam [34]	Moderate	85	0.48	420	96.84
PSO [35]	Good	72	0.61	465	97.32
WOA [36]	Good	68	0.57	452	97.68
ACO [37]	Moderate–Good	75	0.64	478	97.15
CCO	Very Fast	41	0.09	398	99.71

(Proposed)					

Table 9 compares the performance of the various optimization algorithms with respect to convergence rate, number of iterations taken to converge, computation time, memory usage, and the classification accuracy on the various data sets. Adam exhibits moderate convergence as the iterations increase, whereas PSO and WOA have better convergence behavior but need more computational resources. ACO demonstrates consistent optimization performance with a comparatively high memory usage. Conversely, the proposed Cuckoo Catfish Optimizer (CCO) has a high convergence rate of 41 iterations, a low computational time of 0.09 seconds, a low memory consumption of 398 MB, and the best accuracy of 99.71%, which is superior in optimization efficiency and learning stability.

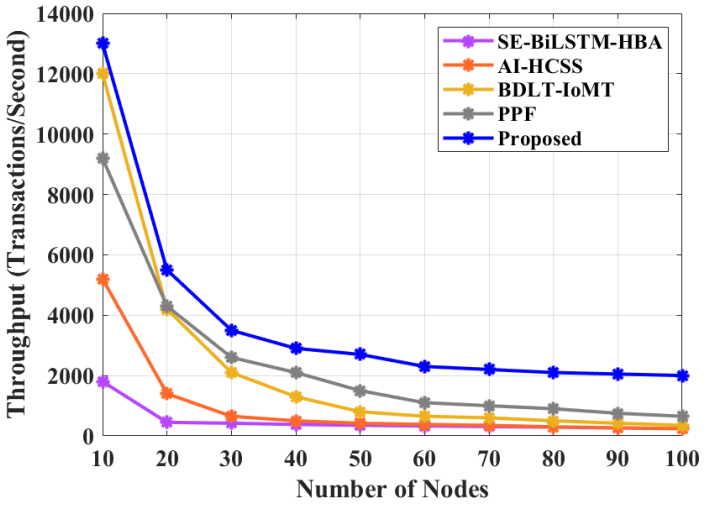


Figure 11: Throughput comparison of blockchain frameworks under varying numbers of network nodes

Figure 11 analyzes the performance of blockchain throughput based on various methods against the increased number of network nodes. The HBC-SGNN offers a greater processing speed of transactions than current methods, which is stable despite the growth in the number of nodes. Scalability and processing bottleneck. Efficacy: Consensus learning and graph-based validation mechanisms enhance efficient consensus learning. The healthcare environments can improve the efficiency of the systems through secure data handling and intelligent validation. The combination of quality ECG classification results with blockchain storage guarantees the consistency and stability of the transaction flow, which emphasizes the relevance of the framework to decentralized medical data management on a large scale and real-time cybersecurity monitoring.

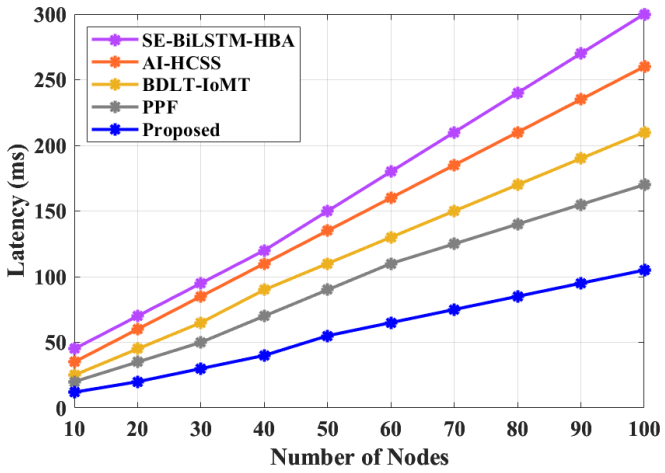


Figure 12: Latency comparison of blockchain systems with increasing network size

Figure 12 represents the comparison of latency between blockchain solutions with the increase in the number of nodes. The suggested HBC-SGNN has a reduced latency increase in the case of existing models, which means that it can confirm transactions faster and respond better. Optimal consensus and effective spectral graph learning minimize communication delays among nodes in a distributed system. The framework guarantees that

ECG data that are strictly classified can be validated and delivered at a very low delay to facilitate real-time healthcare applications. The low latency proves the better scalability and efficiency of operation, affirming that the blockchain-powered cybersecurity system can be kept stable despite the growing complexity of the network.

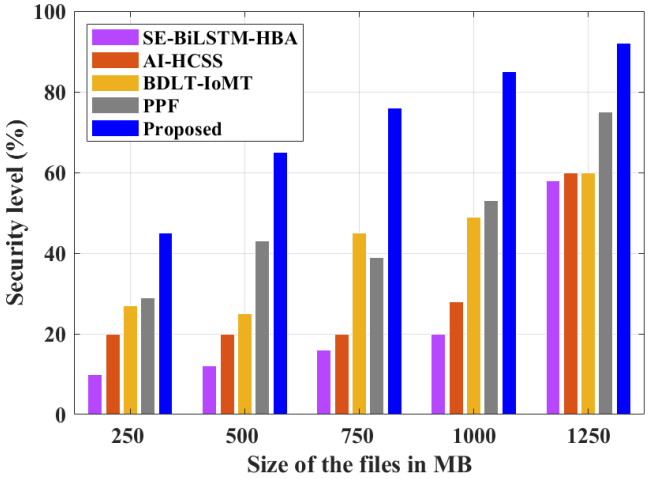


Figure 13: Security level comparison of blockchain frameworks for varying data file sizes

Figure 13 shows the comparison of security levels of various blockchain frameworks with different file sizes. The HBC-SGNN proposed can be more secure because of decentralized validation and smart graph-based attack detection procedures. Since the size of data is large, the framework is highly protective against malicious actions as well as securely storing classified ECG records. Data integrity is improved with blockchain consensus as the optimized learning outputs are integrated to increase resistance to cyber threats. Findings indicate that the framework is effectively balanced in terms of scalability and protection and can be used to exchange healthcare data securely in a distributed medical setting.

4.5 Ablation Study

Ablution study is an experimental analysis technique that is applied to determine the significance of the specific components in a proposed system. It systematically removes or modifies single modules and determines the performance change to determine the contribution of each component. Design decisions can also be justified indirectly through the process, and understanding how the model operates and how the different parts work together to make the system as a whole very effective and reliable.

Table 10: Ablation Study of the Proposed Framework

Model Variant	Acc (%)	Pre (%)	Recall (%)	F1-score (%)	Spec (%)	Security Level (%)
Without JFL-BLRPOP	96.42	96.30	96.25	96.27	96.20	95.80
Without S-STFFT	97.18	97.05	97.02	97.03	96.98	96.45
Without PCA-1DCN	95.74	95.60	95.55	95.57	95.50	95.10
Without CCO	98.63	98.50	98.46	98.48	98.40	97.85
Without HBC-SGNN	98.05	97.92	97.88	97.90	97.82	94.60
Full Proposed Model	99.71	99.64	99.57	99.60	99.59	99.68

Table 10 presents the ablation study that identifies the role of each component in the proposed framework by removing individual modules and then observing the performance change. The results show that a system is less successful in classification without preprocessing and feature extraction steps due to worse signal representations. There is the greatest effect of performance in eliminating the classification network, which shows that it plays an important role in the learning of the ECG pattern process. The lack of optimization decreases efficiency slightly, and the removal of blockchain decreases the level of security to a significant

extent. The whole proposed model leads to the best performance in every indicator, which demonstrates that each module adds to accuracy, robustness, and safe data processing in the healthcare sector.

4.6 Statistical Analysis

The validation method to determine whether any gains observed during an experiment are real and not due to mere chance is statistical significance analysis. It involves hypothesis testing methods to compare the performances of models in terms of the calculated probability values (p-values). When the p-value falls below some pre-defined value, typically 0.05, the improvement is said to be statistically significant. The analysis ensures reliability, reproducibility, and scientific credibility of performance in experimental research in the fields of deep learning and data-driven research.

Table 11: Statistical Significance Analysis of the Proposed Method

Compared Method	Wilcoxon Signed-Rank Test (p-value)	Paired t-Test (p-value)
CNN-VAE [16]	0.0024	0.0031
L5G-Net [17]	0.0027	0.0034
ECG-STAR Net [18]	0.0029	0.0036
KD-CNN [19]	0.0031	0.0038
ResNet [20]	0.0026	0.0033

Table 11 presents a statistical comparison (Wilcoxon signed-rank and paired t-test) of the given framework and the existing ECG classification methods. The p-values of all of the compared models are below the level of significance of 0.05, which implies that the improvement in performance offered by the suggested approach cannot be attributed to a chance change. The paired t-test guarantees consistency in performance enhancement in repeated outcomes of experiments, and the Wilcoxon test corrects the strength in non-normal distributions. These results indicate the validity, repeatability, and high quality of the proposed framework in accurate and stable ECG classification.

4.7 Discussion

The proposed blockchain-based cybersecurity model is an effective and secure ECG classification consisting of several complementary steps. To begin with, JFL-BLRPOP enhances the quality of signals by reducing noise and preserving important cardiac characteristics. The extraction of S-STFFT features gives rich time-frequency representations, and this aspect makes them more useful when trying to discriminate patterns. The PCA-1DCN is an efficient ECG classifier that obtains temporal dependencies and morphological changes of heart signals. The CCO also approximates the model parameters in a better way, promoting the learning process and stability of the convergence. The HBC-SGNN would be applied to ensure the security of data validation, attack detection, and reliable storage in a decentralized environment to improve cybersecurity.The performance of the framework is measured in terms of accuracy, precision, recall, F1-score, specificity, error rate, computational time, latency, throughput, and the level of security of the framework, showing reliable classification, efficient computation, scalability, and secure healthcare data management.

5. Conclusion

The study provides a blockchain-based cybersecurity architecture of deep learning-based ECG classification, which aims to provide accurate cardiac diagnoses and real-time healthcare data security. In the proposed structure, the signal improvement components are combined with JFL-BLRPOP, the informative feature extraction is performed using S-STFFT, the classification is carried out efficiently using PCA-1DCN, and the parameter optimization is achieved by CCO. Moreover, the Holistic Blockchain Consensus Spectral Graph Neural Network (HBC-SGNN) enhances the security of cyberspace by enforcing decentralized authentication, safe storage, and intrusion detection. The key benefits of the framework are high classification reliability, effective computation, high scalability, and good information security with reliable information exchange. Although these are the advantages, the suggested approach has some shortcomings, such as higher computational overheads because of the multi-stage processing and the reliance on high-scale data sets to achieve optimal learning results. Also, integration of blockchain can add communication overhead in resource-constrained settings. Future work will be concerned with the design of lightweight models, real-time edge deployment, adaptive optimization of blockchain consensus, and the generalization of the model to multi-modal biomedical signal analysis and clinical applications with large-scale health care.

References

1. Eleyan, A. and Alboghbaish, E., 2024. Electrocardiogram signals classification using deep-learning-based incorporated convolutional neural network and long short-term memory framework. Computers, 13(2), p.55.

2. Lim, J., Han, D., Nejad, M.P.S. and Chon, K.H., 2024. ECG classification via integration of adaptive beat segmentation and relative heart rate with deep learning networks. Computers in biology and medicine, 181, p.109062.
3. Mantravadi, A., Saini, S., Mittal, S., Shah, S., Devi, S. and Singhal, R., 2024. CLINet: A novel deep learning network for ECG signal classification. Journal of Electrocardiology, 83, pp.41-48.
4. Eleyan, A., AlBoghbaish, E., AlShatti, A., AlSultan, A. and AlDarbi, D., 2024. RHYTHMI: A deep learning-based mobile ECG device for heart disease prediction. Applied System Innovation, 7(5), p.77.
5. Peng, H., Chang, X., Yao, Z., Shi, D. and Chen, Y., 2024. A deep learning framework for ECG denoising and classification. Biomedical Signal Processing and Control, 94, p.106441.
6. Rahman, S., Pal, S., Yearwood, J. and Karmakar, C., 2024. Robustness of Deep Learning models in electrocardiogram noise detection and classification. Computer Methods and Programs in Biomedicine, 253, p.108249.
7. Singh, P.N. and Mahapatra, R.P., 2024. A novel deep learning approach for arrhythmia prediction on ECG classification using recurrent CNN with GWO. International Journal of Information Technology, 16(1), pp.577-585.
8. Kanna, S.R., Murthy, M.Y.B., Gawali, M.B., Rubai, S.M., Reddy, N.S., Brammya, G. and Preetha, N.N., 2024. A deep learning-based disease diagnosis with intrusion detection for a secured healthcare system. Knowledge and Information Systems, 66(9), pp.5669-5707.
9. Almazroi, A.A., 2025. Innovative AI ensemble model for robust and optimized blockchain-based healthcare systems. Network Modeling Analysis in Health Informatics and Bioinformatics, 14(1), p.6.
10. Ma, L. and Zhang, F., 2024. A novel real-time detection and classification method for ECG signal images based on deep learning. Sensors, 24(16), p.5087.
11. Guhdar, M., Mohammed, A.O. and Mstafa, R.J., 2025. Advanced deep learning framework for ECG arrhythmia classification using 1D-CNN with attention mechanism. Knowledge-Based Systems, 315, p.113301.
12. Pachiyannan, P., Alsulami, M., Alsadie, D., Saudagar, A.K.J., AlKhathami, M. and Poonia, R.C., 2024. A novel machine learning-based prediction method for early detection and diagnosis of congenital heart disease using ECG signal processing. Technologies, 12(1), p.4.
13. Han, Y., Han, P., Yuan, B., Zhang, Z., Liu, L. and Panneerselvam, J., 2024. Novel transformation deep learning model for electrocardiogram classification and arrhythmia detection using edge computing. Journal of Grid Computing, 22(1), p.7.
14. Ji, W. and Zhu, D., 2024. ECG classification exercise health analysis algorithm based on GRU and convolutional neural network. IEEE Access, 12, pp.59842-59850.
15. Lamba, S., Kumar, S. and Diwakar, M., 2025. FADLEC: feature extraction and arrhythmia classification using deep learning from electrocardiograph signals. Discover Artificial Intelligence, 5(1), p.82.
16. Selvam, I.J., Madhavan, M. and Kumarasamy, S.K., 2025. Detection and classification of electrocardiography using hybrid deep learning models. Hellenic Journal of Cardiology, 81, pp.75-84.
17. Yang, T., Xie, C.X., Huang, H.M., Wang, Y., Fan, M.H., Kuo, I.C., Chen, T.Y., Chen, S.L., Chen, C.A., Abu, P.A.R. and Wang, L.H., 2025. Lead Analysis for the Classification of Multi-Label Cardiovascular Diseases and Neural Network Architecture Design. Electronics, 14(16), p.3211.
18. Liu, C.L., Xiao, B. and Tsai, C.F., 2025. ECG-STAR: Spatio-temporal attention residual networks for multi-label ECG abnormality classification. Information Sciences, 717, p.122273.
19. Borah, B.B., Das, K., Hazarika, U. and Roy, S., 2024. A deep knowledge distillation heartcare framework for detection of multi-label myocardial infarction from multi-lead ecg signals. SN Computer Science, 6(1), p.14.
20. Cid, F. (2026). Resilient Communication Protocol Design with Integrated Anomaly Detection for Software-Defined Networking Environments. *Transactions on Secure Communication Networks and Protocol Engineering*, 42-49.
21. Alotaibi, J., 2025. A hybrid software-defined networking approach for enhancing IoT cybersecurity with deep learning and blockchain in smart cities. Peer-to-Peer Networking and Applications, 18(3), p.123.
22. Kolsur, S. and Hosmani, S., 2025. Artificial intelligence-based healthcare cybersecurity system with blockchain: modified parallel convolutional neural network for attack detection. Medicine in Novel Technology and Devices, p.100412.
23. Mleh, K. L., Klabi, H., &Sikalu, K. P. (2026). A Mechanobiology-Driven Computational–Experimental Framework for Investigating Cellular Remodeling During Wound Healing. *Frontiers in Life Sciences Research*, 28-38.
24. Patil, S.M., Dakhare, B.S., Satre, S.M. and Pawar, S.D., 2025. Blockchain-based privacy preservation framework for preventing cyberattacks in smart healthcare big data management systems. Multimedia Tools and Applications, 84(22), pp.25547-25566.
25. Tan, H., Xiang, G., Xie, X. and Jia, H., 2024, December. Joint frame-level and block-level rate-perception optimized preprocessing for video coding. In Proceedings of the 6th ACM International Conference on Multimedia in Asia (pp. 1-1).
26. Zhao, Z. and Li, G., 2023. Synchrosqueezing-based short-time fractional Fourier transform. IEEE Transactions on Signal Processing, 71, pp.279-294.

27. Rahim, R. (2026). High-Resolution Spatiotemporal Proteogenomic Profiling Of Host–Pathogen Interactions During Bacterial Infection. *Frontiers in Life Sciences Research*, 1-9.
28. Nasser Alwetaishi and Aziz Alzaed. (2026). Smart Construction Materials for Sustainable and Resilient Infrastructure Innovations. *Innovative Reviews in Engineering and Science*, *3*(2), 60-72.
29. Rajendran, M. (2026). Reduced Order Modeling of Nonlinear Aeroelastic Flutter in Flexible Wing Configurations. *Applied Nonlinearity in Science and Technology*, 35-39.
30. Bertrand, N., Gramoli, V., Konnov, I., Lazić, M., Tholoniat, P. and Widder, J., 2022. Holistic verification of blockchain consensus. arXiv preprint arXiv:2206.04489.
31. Zhang, B., Zhao, L. and Maron, H., 2024. On the expressive power of spectral invariant graph neural networks. arXiv preprint arXiv:2406.04336.
32. Atwa, A.E.M., Atlam, E.S., Ahmed, A., Atwa, M.A., Abdelrahim, E.M. and Siam, A.I., 2025. Interpretable deep learning models for arrhythmia classification based on ecg signals using ptb-x dataset. Diagnostics, 15(15), p.1950.
33. Abid, Y.A., Wu, J., Xu, G., Fu, S. and Waqas, M., 2024. Multilevel deep neural network approach for enhanced distributed denial-of-service attack detection and classification in software-defined Internet of Things networks. IEEE Internet of Things Journal, 11(14), pp.24715-24725.
34. Sun, H., Zhou, W., Yang, J., Shao, Y., Xing, L., Zhao, Q. and Zhang, L., 2024. An improved medical image classification algorithm based on Adam optimizer. Mathematics, 12(16), p.2509.
35. Kannan, S.K. and Diwekar, U., 2024. An enhanced particle swarm optimization (PSO) algorithm employing quasi-random numbers. Algorithms, 17(5), p.195.
36. Zhou, Y. and Hao, Z., 2025. Multi-strategy improved whale optimization algorithm and its engineering applications. Biomimetics, 10(1), p.47.
37. Cui, J., Wu, L., Huang, X., Xu, D., Liu, C. and Xiao, W., 2024. Multi-strategy adaptable ant colony optimization algorithm and its application in robot path planning. Knowledge-Based Systems, 288, p.111459.